

# Wood/Polymer Nanocomposites Prepared by Impregnation with Furfuryl Alcohol and Nano-SiO<sub>2</sub>

Youming Dong,<sup>a,b,c,#</sup> Yutao Yan,<sup>a,b,c,#</sup> Shifeng Zhang,<sup>a,b,c,\*</sup> and Jianzhang Li<sup>a,b,c,\*</sup>

Wood/polymer nanocomposites were prepared by vacuum impregnation of furfuryl alcohol (FA) and nano-SiO<sub>2</sub> into fast-growing poplar wood. The nano-SiO<sub>2</sub> was mixed with FA solution, followed by *in-situ* polymerization of FA. The properties of nanocomposites and the effects of nanoparticles on these properties were investigated. Wood physico-mechanical properties, such as dimensional stability, density, water uptake, and surface hardness, were significantly improved. Moreover, the addition of nano-SiO<sub>2</sub> improved the surface hardness and dimensional stability of wood and kept the excellent properties of FA-treated wood. Thermogravimetric analysis indicated that the effect of nano-SiO<sub>2</sub> on thermostability was hindered. X-ray photoelectron spectroscopy and scanning electron microscopy with energy-dispersive X-ray spectroscopy showed that nano-SiO<sub>2</sub> was successfully incorporated into wood *via* the action of FA, and diffused into the wood lumen and cell wall. X-ray diffraction results indicated the weakening of the crystallinity in the treated wood was due to the polymerization of FA.

**Keywords:** Renewable resources; Wood/polymer nanocomposite (WPNC); Wood modification; Furfurylation; Nano-SiO<sub>2</sub>

**Contact information:** a: MOE Key Laboratory of Wooden Material Science and Application; b: Beijing Key Laboratory of Wood Science and Engineering; c: MOE Engineering Research Center of Forestry Biomass Materials and Bioenergy, Beijing Forestry University, Beijing 100083, China; <sup>#</sup>These authors contributed to this work equally;

\* Corresponding authors: zhangshifeng2013@126.com; lijianzhang126@126.com

## INTRODUCTION

Environmental and economic concerns have opened new opportunities for the development of wood modification. Many processes have been published in this field (Rowell 2005). The widely studied processes include acetylation, furfurylation, impregnation with lower molecular weight resins, cross-linking modification, and thermal modification (Deka and Saikia 2000; Lande *et al.* 2008; Esteves and Pereira 2009; Li *et al.* 2009; Cetin *et al.* 2011).

The application of biomass-derived substances for wood modification has the potential to reduce the depletion of petroleum resources. Among the biomass-derived chemicals, furfuryl alcohol (FA) derived from renewable saccharidic resources is an attractive intermediate for various useful polymer products (Moreau *et al.* 2004; Kim *et al.* 2014). With many advantages and development prospects, wood furfurylation becomes an excellent method in wood modification. This process is based on wood impregnation with FA and other agents, followed by *in-situ* polymerization at an elevated temperature. After decades of development, many properties of furfurylated wood have been studied, such as dimensional stabilization (Stamm 1977; Baysal *et al.* 2004), physico-mechanical properties (Schneider *et al.* 2000), moisture content (Thygesen and

Elder 2009), durability (De Vetter *et al.* 2009), and ecotoxicity (Lande *et al.* 2004). These studies show that furfurylated wood is an excellent and eco-friendly material, and consequently, it has been successfully commercialized. The furfurylated wood has been applied to construction materials, furniture, and flooring products (Lande *et al.* 2008). Moreover, many studies have focused on the mechanisms of FA polymerization (Choura *et al.* 1996; Nordstierna *et al.* 2008). Although many properties of wood can be improved by furfurylation, the enhancement of mechanical strength is not notable with a low weight percent gain (WPG), especially the modulus of elasticity (MOE), impact strength, and bending strength, which are important in wood applications. Moreover, the wood becomes darker after furfurylation (Herold *et al.* 2013), which also limits the application of this process. Hence, it is significant to investigate how to improve the wood strength with low WPG and alleviate discoloration, especially in fast-growing wood.

Nano-based treatments applied to wood modification present new opportunities to enhance wood properties. Wood polymer nanocomposites (WPNC) can be prepared with a range of improved physical, mechanical, and other properties. Many attempts have been made in this field in the past decades. A WPNC was prepared using water-soluble phenolic resin (PF) and montmorillonite (MMT) with improved surface mechanical properties, flame retardance, and dimensional stability (Xue and Zhao 2008). Solid aspen wood properties were improved, including surface hardness, MOE, dimensional stability, and water resistance, by impregnating wood with melamine-urea-formaldehyde (MUF) in combination with MMT (Cai *et al.* 2008). The impregnation of wood with urea formaldehyde (UF) and nano-SiO<sub>2</sub> improved the dimensional stability, flame resistance, and hardness (Shi *et al.* 2007). A WPC was prepared on the basis of nano-SiO<sub>2</sub> and nanoclay by impregnation of melamine formaldehyde-FA copolymer, and many properties were improved (Hazarika and Maji 2013).

Nano-SiO<sub>2</sub> is widely used in polymer composites to improve the mechanical strength and can be also applied to improve the properties of FA-modified wood. These organic/inorganic hybrid materials combine the properties of organic polymers and inorganic ceramics. In poly-furfuryl alcohol (PFA)/SiO<sub>2</sub> hybrid material, the nano-SiO<sub>2</sub> can restrict the motions of the furan chains and thus improve the internal rigidity and thermal stability of the organic/inorganic system (Guigo *et al.* 2009). Therefore, the PFA/SiO<sub>2</sub> hybrid material endows the wood with high mechanical strength and thermal stability.

With this in mind, we evaluated the feasibility of preparing wood polymer nanocomposites from furfurylated wood with nano-SiO<sub>2</sub>. In addition, the location of PFA and nano-SiO<sub>2</sub> in the wood and the effects of nano-SiO<sub>2</sub> on properties of the wood were also investigated.

## EXPERIMENTAL

### Materials

Defect-free and straight-grained sapwood of fast-growing poplar wood (*Populus* spp.) was obtained from Guangxi Gaofeng Forest Farm, China. End-matched samples for both the modified and control samples were manufactured with a dimension of 20 mm × 20 mm × 20 mm. To reduce deviation, all samples were chosen from the same timber and machined (sawn and planed) at the same time.

Furfuryl alcohol (chemical purity 98.0%; Sinopharm Chemical Reagent Co., Ltd., China), nano-SiO<sub>2</sub> (particle diameter: 15 ± 5 nm; Shanghai Maikun Chemical Co., Ltd., China), maleic anhydride, and disodium tetraborate (analytically pure, Beijing Chemical Works, China) were used in these studies.

## Methods

### *Preparation of impregnation solutions*

Two types of impregnation solutions were prepared: 50 wt% FA water solution; and 50 wt% FA water solution containing 1.0 wt% nano-SiO<sub>2</sub> (mixed by sonication for 30 min). These dispersions were used for impregnation after the addition of 2 wt% maleic anhydride and 4 wt% disodium tetraborate.

### *Furfurylation*

Samples were impregnated with FA and nano-SiO<sub>2</sub> *via* the following procedures. Drying: The samples were initially dried at 105 °C until reaching constant weight. Afterwards, the dimensions and weights were measured.

Impregnation: The samples were immersed in the solution using a vacuum drying oven (0.1 bar vacuum, 60 min). After impregnation, the excessive solution from the samples was blotted with tissue paper.

Polymerization: The samples were wrapped with aluminum foil, kept at room temperature for 12 h, and placed into an oven at 100 °C for another 12 h for polymerization. Afterwards, the aluminum foil was removed and the sample was dried at 105 °C until constant weight was obtained. The dimensions and weights were then measured. The WPG and 24 h deionized water immersion leachability (*L*) were calculated as follows:

$$\text{WPG (\%)} = (W_1 - W_0)/W_0 \times 100 \quad (1)$$

$$L (\%) = (W_1 - W_3)/(W_1 - W_0) \times 100 \quad (2)$$

where *W*<sub>0</sub> and *W*<sub>1</sub> are the oven-dried weights of a specimen before treatment and after treatment, respectively, and *W*<sub>3</sub> is the oven-dried weights of treated samples after 24 h of water immersion.

### *X-ray photoelectron spectroscopy (XPS) analysis*

The presence of silicon deposits in the samples were investigated by XPS (K-Alpha Thermo Scientific, USA) with a monochromatic Al Kα X-ray source at a pressure of 10<sup>-8</sup> mbar. Survey spectra were recorded with 1.0-eV steps and 200-eV analyzer pass energy, and high resolution regions were investigated with 0.1-eV steps and 50-eV pass energy. The spot size was roughly 400 μm<sup>2</sup>. All binding energies were calibrated with the C1s peak at 285 eV as a reference, which corresponds to the carbons in aromatic hydrocarbons. The ratio of elemental silica to carbon (Si/C) was determined from the low-resolution spectra.

***Scanning electron microscopy (SEM) and energy-dispersive X-ray spectroscopy (EDX)***

The penetration ability of PFA resin with nano-SiO<sub>2</sub> into the cell wall and its distribution within the cell wall were analyzed using SEM (Hitachi S-3400N, Japan). Therefore, tangential and radial sections of treated and untreated wood samples were mounted on conductive adhesives, sputter-coated with gold, and then observed under SEM at an accelerating voltage of 15 kV. In addition, the wood samples were also analyzed by SEM (Hitachi S-4800, Japan) coupled with energy dispersive X-ray analysis (EDX).

***Fourier transform infrared spectrometry (FT-IR)***

The treated and untreated wood samples were milled to a 200-mesh particle size and embedded into potassium bromide (KBr) pellets at a ratio of 1:100 in weight. The pellets were analyzed by FT-IR (Nicolet 6700 Thermo Scientific, USA) with a scanning range of 4000 to 400 cm<sup>-1</sup> at a resolution of 4 cm<sup>-1</sup> for 32 scans.

***X-ray diffraction (XRD) analysis***

The crystallinity of the treated and untreated wood samples was evaluated by XRD, using an XRD 6000 diffractometer (Shimadzu, Japan). The apparatus parameters were as follows: Cu K $\alpha$  radiation with graphite monochromator, voltage 40 kV, electric current 30 mA and 2 $\theta$  scan range of 5 to 40° with a scanning speed of 2° min<sup>-1</sup>.

***Measurement of physical and mechanical properties***

Dimensional stability was evaluated by measurement of anti-swelling efficiency (ASE) as follows:

$$\text{ASE (\%)} = (S_u - S_t) / S_u \times 100 \quad (3)$$

where  $S_u$  is the volumetric swelling of an untreated sample and  $S_t$  is that of a treated sample.

Water uptake (WU) after 24 h of deionized water immersion and bulking effect (BE) were calculated as follows:

$$\text{WU (\%)} = (W_2 - W_1) / W_1 \times 100 \quad (4)$$

$$\text{BE (\%)} = (V_1 - V_0) / V_0 \times 100 \quad (5)$$

where  $W_2$  is the weight of a wood sample after 24 h water immersion, and  $V_0$  and  $V_1$  are the dried wood volumes before and after treatment, respectively.

Surface hardness was measured with a TH210 durometer (Beijing TIME High Technology Ltd., China) and expressed as Shore D hardness according to ASTM D2240 (2010). Each type of sample was measured by 20 tests.

***Thermogravimetric Analysis (TGA)***

Thermal stabilities of the untreated and treated wood samples were evaluated by TGA, using a Q5000 TGA analyzer (TA Instruments, USA) at a constant heating rate of 20 °C min<sup>-1</sup> from room temperature to 600 °C under a flowing nitrogen atmosphere.

## RESULTS AND DISCUSSION

After treatment, the WPNC was prepared with an even color distribution (*i.e.*, dark brown) from the exterior to the interior in the longitudinal section. Figure 1 shows the exterior and the interior of the untreated or treated wood with FA and FA/SiO<sub>2</sub>. The average WPGs is 73.98% for the FA-treated wood and 76.47% for the FA/SiO<sub>2</sub>-treated wood. The dark color is generated by the conjugated structure derived from the aliphatically linked PFA (Choura *et al.* 1996). Although the WPG of the FA/SiO<sub>2</sub>-treated wood was higher than the FA-treated wood, its color was lighter, which is likely due to the conjugation confinement of nano-SiO<sub>2</sub> network in the PFA. The average leachabilities of the FA-treated and the FA/SiO<sub>2</sub>-treated samples were both less than 6.2%.



**Fig. 1.** Color of untreated and treated wood samples. Inside color: (a<sub>1</sub>) untreated wood; (b<sub>1</sub>) FA-treated wood; and (c<sub>1</sub>) FA/SiO<sub>2</sub>-treated wood. Surface color: (a<sub>2</sub>) untreated wood; (b<sub>2</sub>) FA-treated wood; and (c<sub>2</sub>) FA/SiO<sub>2</sub>-treated wood

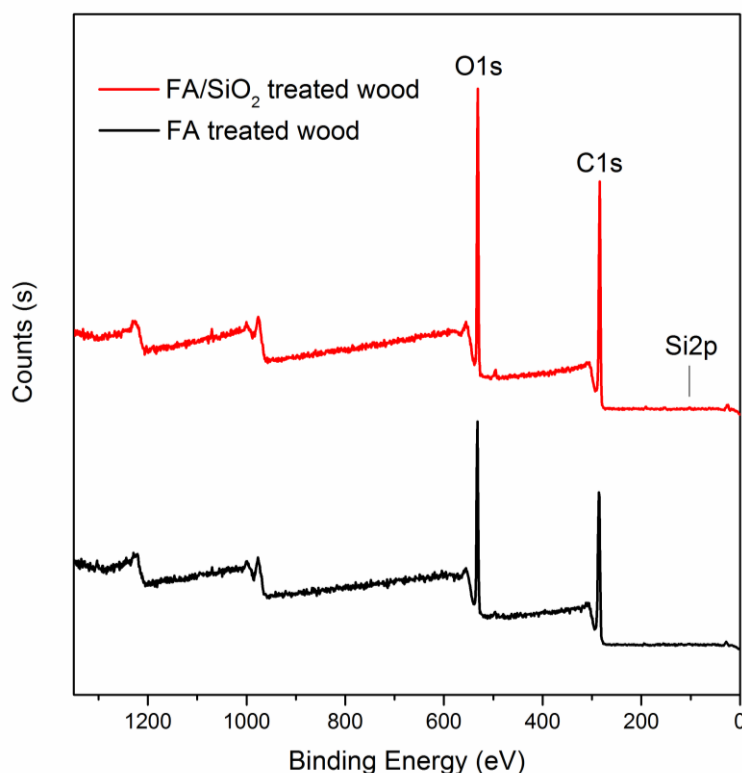


**Fig. 2.** Survey XPS spectra of FA/SiO<sub>2</sub>-treated and FA-treated samples

## XPS Analysis

Figure 2 shows the typical XPS survey spectra for the treated wood samples. Inspection of these XPS spectra revealed that the C and Si occurred at 285 eV and 102 eV, respectively. For the FA/SiO<sub>2</sub>-treated wood, the absolute differences in mol% were 97.8 and 2.2 At% (atom percentage) for C and Si, respectively, and the Si/C ratio was 0.0225. In comparison, the absolute differences of FA-treated wood were 98.38 and 1.61 At% for C and Si, respectively, and the Si/C ratio was 0.0164. The very small Si content of natural poplar wood concurs with the results of a previous study (Liao *et al.* 2004). Obviously, the Si content in the FA/SiO<sub>2</sub>-treated wood was higher when compared with the FA-treated wood, which indicated the successful incorporation of nano-SiO<sub>2</sub> into the wood.

## SEM Analysis

Figure 3 shows the morphologies of the untreated wood and the wood treated with FA or FA/SiO<sub>2</sub> at different magnifications. Empty cell walls, pits, and distinct lacunae were obvious in the untreated wood (Fig. 3a), while these empty places in the treated wood were occupied by the resin or nano-SiO<sub>2</sub> materials. Noticeably, the wood vessel walls were rough and the pits were filled with polymer, with many distinct wavy structures on the walls (Fig. 3b). These changes were due to the polymerization of FA. However, no notable polymer aggregation occurred on the surface, probably because the morphology of PFA is glasslike, and the polymer is well-distributed in the wood cell walls (Fitzer *et al.* 1969). It was deduced from these observations that the PFA was in intimate contact with the wood cell walls.

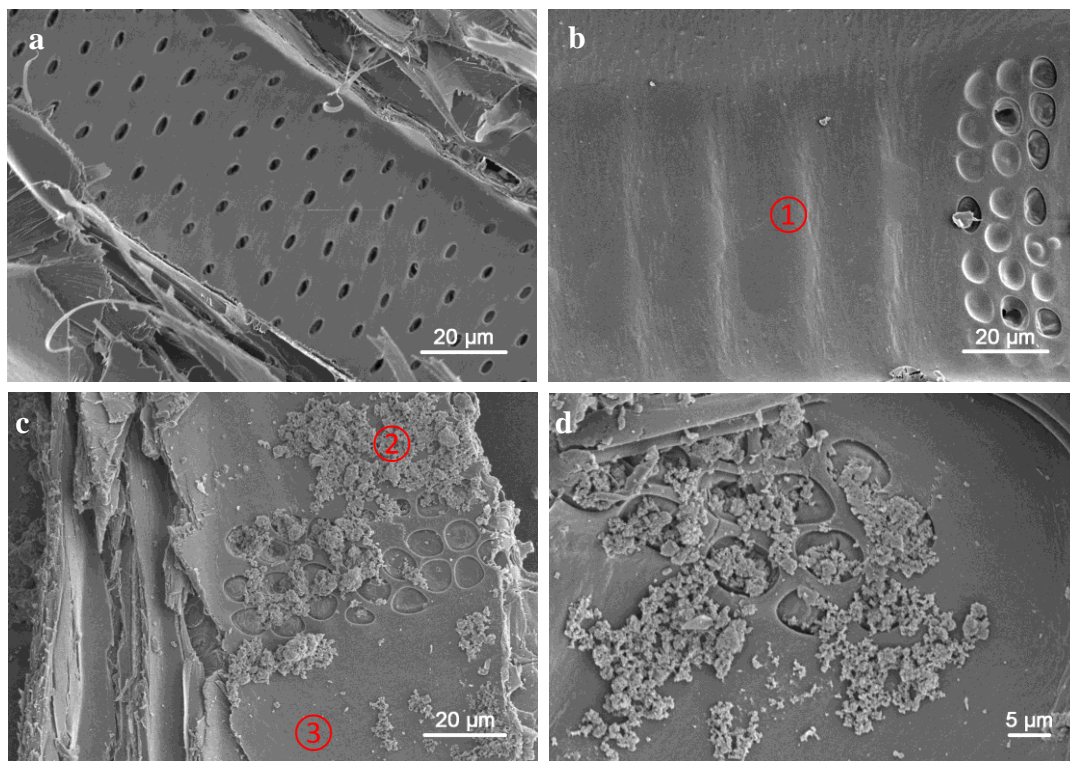


**Fig. 3.** Scanning electron micrographs: (a) untreated; (b) FA-treated; and (c) and (d) FA/SiO<sub>2</sub>-treated wood samples

With the addition of nano-SiO<sub>2</sub> into the FA solution, many clusters adhered to the cell walls and even plugged the pits of the treated wood (Figs. 3c and 3d). With the presence of nanopores, wood can accommodate nanoparticles (Xue and Zhao 2008). Hence, these clusters could be a part of nano-SiO<sub>2</sub> particles that cannot enter the wood cell walls due to its agglomeration and separate from PFA. The diameter of these inorganic clusters was about 5 μm. These observations supported the XPS data. In addition, a part of the nanoparticles was covered by PFA resin (Fig. 3c), indicating that the nano-SiO<sub>2</sub> can be incorporated with FA to form a composite material. In general, the effect of the nanoparticles on wood properties may be noticeable.

By SEM-EDX, the elemental composition of the FA- and FA/SiO<sub>2</sub>-treated wood samples was determined, and the results are shown in Table 1. For the data of point 2, it can be determined that the agglomerates were comprised of SiO<sub>2</sub>. Comparing the data between point 1 and 3, the distinct difference observed was a unique silicon signal in FA/SiO<sub>2</sub>-treated wood sample. But the amount of silicon was low, which was coincident with the results of XPS. Also, little amounts of sodium were determined in both FA- and FA/SiO<sub>2</sub>-treated wood samples, which was due to the disodium tetraborate in the FA solutions.

**Table 1.** SEM-EDX Values of Carbon, Oxygen, and Silicon in Points 1, 2, and 3 in Fig. 3b and c

Point	Carbon (wt%)	Oxygen (wt%)	Silicon (wt%)
1	52.97	47.03	0
2	53.83	35.77	10.40
3	51.58	46.92	0.79

### FT-IR Analysis

Figure 4 shows the FT-IR spectra of the four samples over the 400 to 4000 cm<sup>-1</sup> wavenumber range. For the wood samples, the prominent band at 3400 cm<sup>-1</sup> is attributed to the stretching of the -OH, the band at 1730 cm<sup>-1</sup> is assigned to C=O stretching of the acetyl group, the bands at 1596 and 1507 cm<sup>-1</sup> are assigned to the aromatic skeletal vibration of lignin, and the band at 1261 cm<sup>-1</sup> is assigned to C–O stretching of the guaiacyl ring (Pandey 1999). Two notable peaks at 1716 and 1562 cm<sup>-1</sup> only appeared in the treated woods, which are attributed to the C=O stretching vibration of the γ-diketone formed from hydrolytic ring opening of the furan of PFA and the skeletal vibration of 2,5-disubstituted furan rings, respectively (Chuang *et al.* 1984; Pranger and Tannenbaum 2008; Ahmad *et al.* 2013). This result also indicated the polymerization of the FA monomer in the wood. Two small bands at 1652 and 899 cm<sup>-1</sup> in curve b are assigned to the conjugated carbonyl stretching and the β-glucosidic linkages between the sugar units, respectively, whereas they disappeared in both curve c and d (Kačuráková *et al.* 1998; Sun *et al.* 2001). This phenomenon may be attributed to the acid hydrolysis of lignin and hemicellulose in the poplar wood (Lee and McCaskey 1983; Sun *et al.* 2013). The absorption bands in the spectra of two treated woods were not different due to the low amount of SiO<sub>2</sub> particle impregnation, which indicated that the FA was successfully polymerized in the presence of nano-SiO<sub>2</sub> and that no chemical interaction occurred between the SiO<sub>2</sub> and the FA or between the SiO<sub>2</sub> and the wood.

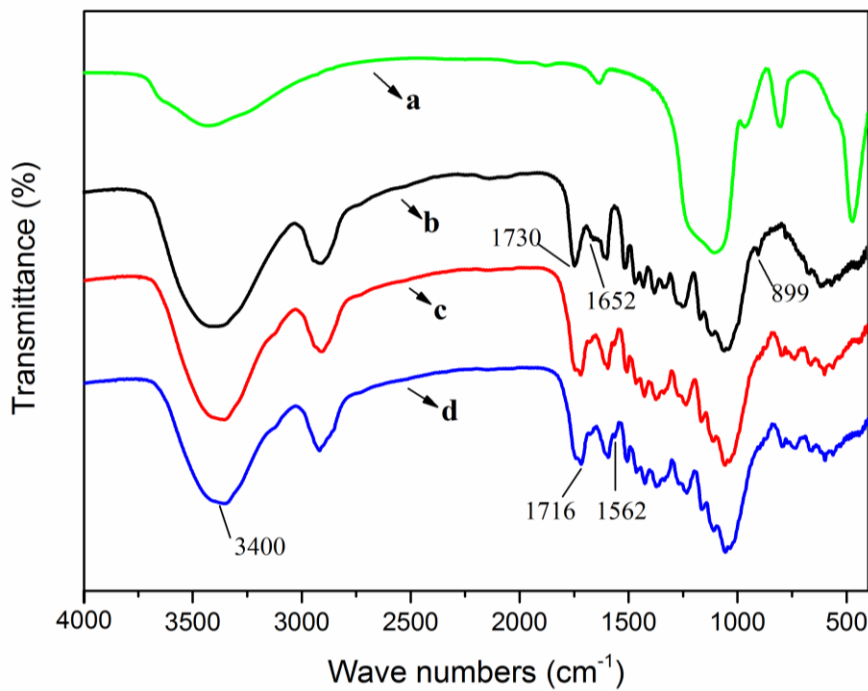


**Fig. 4.** FT-IR spectra: (a) nano-SiO<sub>2</sub>; (b) untreated wood; (c) FA-treated wood; and (d) FA/SiO<sub>2</sub>-treated wood

### XRD Analysis

Figure 5 shows the XRD spectra of untreated-wood, as well as wood treated with water, FA, or FA/SiO<sub>2</sub>. For both untreated and water-treated woods, the XRD peaks mainly occurred at diffraction angles of 16.8°, 22.2°, and 34.6°, and are attributed to the cellulose crystal planes I<sub>101</sub>, I<sub>002</sub>, and I<sub>040</sub>, respectively. Moreover, an obvious trough, which is a characteristic of the amorphous wood region, appeared at 18.2° (Cave 1997). However, the patterns of FA- and FA/SiO<sub>2</sub>-treated woods were substantially changed, with the trough at 18.2° obviously elevated. There was no noticeable difference in the diffractogram of the FA-treated wood with the addition of nano-SiO<sub>2</sub> particles. The difference of peaks at 37.8° may be due to some signal extraneous to the wood composition, and it had little impact on the results. According to a previous report by Zavadskii (2004), the crystallinity of untreated wood was 37.75%, which increased to 46.30% after the wood's treatment with water. In the present furfurylation after 12 h of cure time, the hot water treatment led to rearranged or reoriented cellulose molecules or the crystallization in quasicrystalline of the amorphous region (Bhuiyan *et al.* 2000; Howell *et al.* 2011). The same phenomenon occurred in the FA- or FA/SiO<sub>2</sub>-treated wood. Specifically, the crystallinities of FA- and FA/SiO<sub>2</sub>-treated woods were 42.29% and 43.83% respectively, which indicated that the addition of SiO<sub>2</sub> into the wood slightly increased the crystallinity. The decreased crystallinity in the FA-treated wood when compared to the water-treated wood may be attributed to the amorphous structure of PFA. The FA monomer entered the amorphous region of the cellulose and polymerized *in situ*, which resulted in the swelling of the amorphous region. From this observation, the efficiency of furfurylation may be mainly a filling action, though the grafting between PFA and wood revealed using some model compounds could increase the crystallinity (Nordstierna *et al.* 2008; Wu *et al.* 2010).

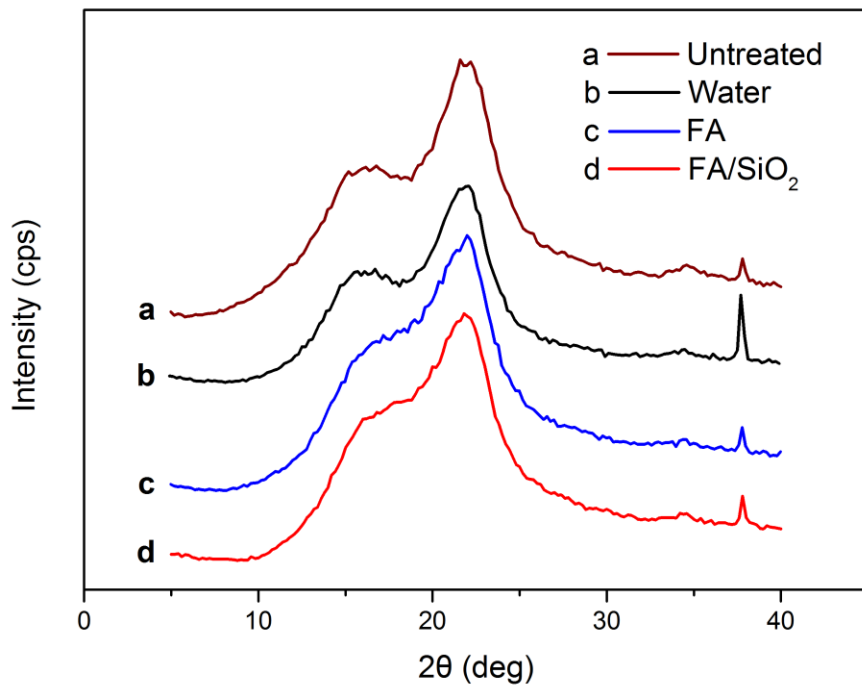


**Fig. 5.** XRD spectra: (a) untreated wood; (b) water-treated wood; (c) FA-treated wood; and (d) FA/SiO<sub>2</sub>-treated wood

### Evaluation of Physical and Mechanical Properties

Table 2 shows the results for the bulk effect (BE), the water uptake (WU), the anti-swelling efficiency (ASE), and the surface hardness of the untreated and treated wood samples. Compared to the untreated wood, the BE, ASE, and surface hardness of the treated wood samples were augmented, while the WU was reduced by about 60%, which was attributed to the over bulking as well as the obstruction of cell wall pits by the hydrophobic PFA. In the FA/SiO<sub>2</sub>-treated wood, the addition of nano-SiO<sub>2</sub> also slightly affected the dimensional stability and surface hardness, suggests that the silica cage restrict the segmental motion of furan chains *via* nanoconfinement and this organic/inorganic hybrid material improves the internal rigidity of the nanocomposite (Guigo *et al.* 2009).

**Table 2.** Physical and Mechanical Properties of Untreated and Treated Wood Samples

Wood sample	BE <sup>a</sup> (%)	WU <sup>a</sup> (%)	ASE <sup>a</sup> (%)	Hardness <sup>b</sup> (Shore D)
Untreated*	2.99 ( $\pm 0.40$ )	113.32 ( $\pm 7.88$ )	0 ( $\pm 2.99$ )	46.97 ( $\pm 4.25$ )
FA-treated	15.02 ( $\pm 1.08$ )	44.55 ( $\pm 5.55$ )	65.75 ( $\pm 0.86$ )	63.14 ( $\pm 4.35$ )
FA/SiO <sub>2</sub> -treated	15.38 ( $\pm 0.33$ )	41.38 ( $\pm 3.68$ )	68.67 ( $\pm 1.72$ )	69.28 ( $\pm 3.45$ )

<sup>a</sup>Each value represents the average of six samples  $\pm$  standard deviation

<sup>b</sup>Each value represents the average of twenty samples

\*Treated with water

## Evaluation of Thermal Stability

Thermal stability of the untreated and treated wood samples was studied using TGA. Figure 6 shows the mass loss of these samples as a function of temperature. The thermal degradation profiles revealed that most of the degradation events occurred between 200 and 400 °C. For the untreated wood, the first degradation region from 50 to 120 °C is related to the release of moisture and adsorbed water from the wood. The weight loss of the treated wood is lower at this temperature range, which implies that the water uptake of the wood was reduced after its modification. This finding also agrees with the previous results of the water uptake test. The untreated wood did not lose more than 20% of its weight before leveling off at 300 °C, whereas the weight of the treated wood distinctly declined from 200 to 300 °C, which was mainly attributed to the thermo-degradation of PFA (Guigo *et al.* 2009).

The main pyrolysis process occurred at 366 °C in the untreated wood and at 333 °C in the FA-treated wood, and slightly higher in the FA/SiO<sub>2</sub>-treated wood than the FA-treated wood. However, the nano-SiO<sub>2</sub> treatment did not noticeably affect the thermal stability of the composites, probably because the high WPG hindered the efficacy of the nano-SiO<sub>2</sub>. The SEM micrographs showed that a large part of nano-SiO<sub>2</sub> may be separated from the PFA by the cell wall, and the synergistic effect of nano-SiO<sub>2</sub> and furanic matrix cannot work. This may be an alternative explanation for the observed result. Because of the high carbon content of PFA, the residual weight for the treated wood was almost two times higher than that of the untreated wood.

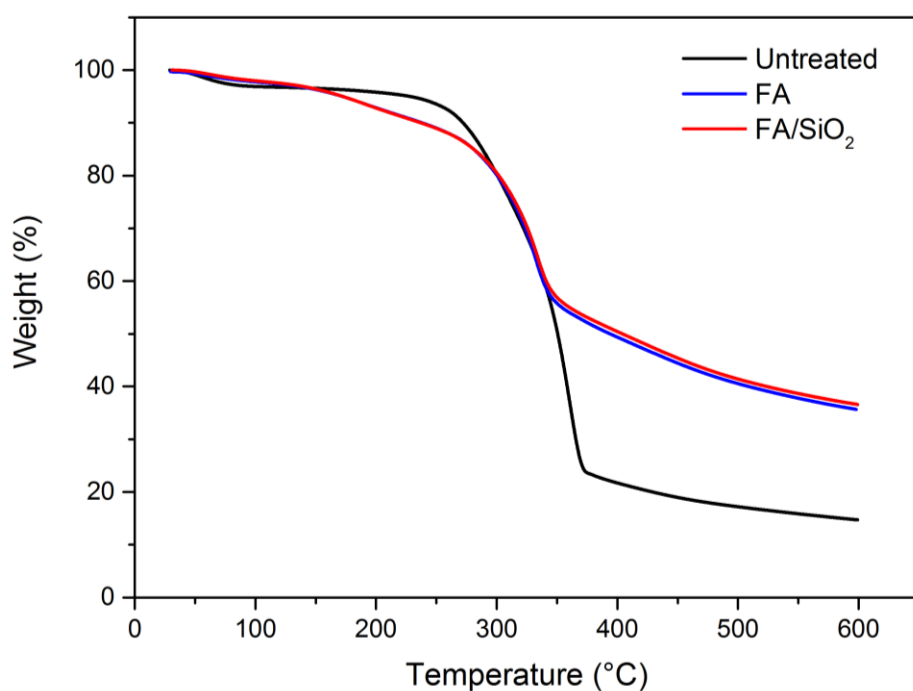


**Fig. 6.** TGA curves of untreated, FA-treated, and FA/SiO<sub>2</sub>-treated wood

## CONCLUSIONS

1. Wood-polymer nanocomposites (WPNC) were successfully prepared from fast-growing poplar wood by impregnation using furfuryl alcohol (FA) and nano-SiO<sub>2</sub>. This process of WPNC using FA and SiO<sub>2</sub> is feasible for the preparation of an effective product with improved properties.
2. SEM-EDX and XPS analyses showed that the nano-SiO<sub>2</sub> was incorporated into wood and diffused in the wood lumen and cell walls when using a FA solution as the medium. The FT-IR results indicated that successful polymerization of FA in wood occurred. However, there was no evidence found for the reaction among the SiO<sub>2</sub>, wood, and FA from the FT-IR analysis.
3. The crystallinity of the FA-treated and FA/SiO<sub>2</sub>-treated composites decreased relative to the untreated wood, as measured by XRD; this may be attributed to the penetration of PFA into the amorphous region of the wood cell wall. Wood properties such as surface hardness, water uptake, and anti-swelling efficiency were improved. The addition of nano-SiO<sub>2</sub> can enhance the dimensional stability and surface hardness of FA-treated wood. The TGA analysis showed that FA/SiO<sub>2</sub> treatment hindered the thermal stability of the wood composite. A more effective process for incorporating nano-SiO<sub>2</sub> and PFA into the wood substrate should be investigated.

## ACKNOWLEDGMENTS

The authors are very grateful for financial support from Special Fund for Forestry Research in the Public Interest (Project 201204702), the Fundamental Research Funds for the Central Universities (TD2011-12) and the National Natural Science Foundation of China (Project 31000268/C160302).

## REFERENCES CITED

- ASTM D2240. (2010). "Standard test method for rubber property-durometer hardness," *ASTM International*, West Conshohocken, PA.
- Ahmad, E. E. M., Luyt, A. S., and Djoković, V. (2013). "Thermal and dynamic mechanical properties of bio-based poly(furfuryl alcohol)/sisal whiskers nanocomposites," *Polym. Bull.* 70(4), 1265-1276.
- Baysal, E., Ozaki, S. K., and Yalinkilic, M. K. (2004). "Dimensional stabilization of wood treated with furfuryl alcohol catalysed by borates," *Wood Sci. Technol.* 38(6), 405-415.
- Bhuiyan, M. T. R., Hirai, N., and Sobue, N. (2000). "Changes of crystallinity in wood cellulose by heat treatment under dried and moist conditions," *J. Wood Sci.* 46(6), 431-436.
- Cai, X., Riedl, B., Zhang, S., and Wan, H. (2008). "The impact of the nature of nanofillers on the performance of wood polymer nanocomposites," *Compos. Part A - Appl. Sci.* 39(5), 727-737.
- Cave, I. (1997). "Theory of X-ray measurement of microfibril angle in wood," *Wood Sci. Technol.* 31(4), 225-234.

- Cetin, N. S., Özmen, N., and Birinci, E. (2011). "Acetylation of wood with various catalysts," *J. Wood Chem. Technol.* 31(2), 142-153.
- Choura, M., Belgacem, N. M., and Gandini, A. (1996). "Acid-catalyzed polycondensation of furfuryl alcohol: Mechanisms of chromophore formation and cross-linking," *Macromolecules* 29(11), 3839-3850.
- Chuang, I. S., Maciel, G. E., and Myers, G. E. (1984). "Carbon-13 NMR study of curing in furfuryl alcohol resins," *Macromolecules* 17(5), 1087-1090.
- De Vetter, L., Stevens, M., and Van Acker, J. (2009). "Fungal decay resistance and durability of organosilicon-treated wood," *Int. Biodeter. Biodegr.* 63(2), 130-134.
- Deka, M., and Saikia, C. (2000). "Chemical modification of wood with thermosetting resin: Effect on dimensional stability and strength property," *Bioresour. Technol.* 73(2), 179-181.
- Esteves, B. M., and Pereira, H. M. (2009). "Wood modification by heat treatment: A review," *BioResources* 4(1), 370-404.
- Fitzer, E., Schaefer, W., and Yamada, S. (1969). "The formation of glasslike carbon by pyrolysis of polyfurfuryl alcohol and phenolic resin," *Carbon* 7(6), 643-648.
- Guigo, N., Mija, A., Zavaglia, R., Vincent, L., and Sbirrazzuoli, N. (2009). "New insights on the thermal degradation pathways of neat poly(furfuryl alcohol) and poly(furfuryl alcohol)/SiO<sub>2</sub> hybrid materials," *Polym. Degrad. Stab.* 94(6), 908-913.
- Hazarika, A., and Maji, T. K. (2013). "Study on the properties of wood polymer nanocomposites based on melamine formaldehyde-furfuryl alcohol copolymer and modified clay," *J. Wood Chem. Technol.* 33(2), 103-124.
- Herold, N., Dietrich, T., Grigsby, W. J., Franich, R. A., Winkler, A., Buchelt, B., and Pfriem, A. (2013). "Effect of maleic anhydride content and ethanol dilution on the polymerization of furfuryl alcohol in wood veneer studied by differential scanning calorimetry," *BioResources* 8(1), 1064-1075.
- Howell, C., Hastrup, A. C. S., Jara, R., Larsen, F. H., Goodell, B., and Jellison, J. (2011). "Effects of hot water extraction and fungal decay on wood crystalline cellulose structure," *Cellulose* 18(5), 1179-1190.
- Kačuráková, M., Belton, P. S., Wilson, R. H., Hirsch, J., and Ebringerová, A. (1998). "Hydration properties of xylan-type structures: An FTIR study of xylooligosaccharides," *J. Sci. Food Agr.* 77(1), 38-44.
- Kim, T., Assary, R. S., Pauls, R. E., Marshall, C. L., Curtiss, L. A., and Stair, P. C. (2014). "Thermodynamics and reaction pathways of furfuryl alcohol oligomer formation," *Catal. Comm.* 46, 66-70.
- Lande, S., Eikenes, M., and Westin, M. (2004). "Chemistry and ecotoxicology of furfurylated wood," *Scand. J. Forest Res.* 19(sup5), 14-21.
- Lande, S., Westin, M., and Schneider, M. (2008). "Development of modified wood products based on furan chemistry," *Mol. Cryst. Liq. Cryst.* 484(1), 367-378.
- Lee, Y., and McCaskey, T. (1983). "Hemicellulose hydrolysis and fermentation of resulting pentoses to ethanol," *TAPPI J.* 66(5), 102-107.
- Li, J. Z., Furuno, T., Zhou, W. R., Ren, Q., Han, X. Z., and Zhao, J. P. (2009). "Properties of acetylated wood prepared at low temperature in the presence of catalysts," *J. Wood Chem. Technol.* 29(3), 241-250.
- Liao, C. P., Wu, C. Z., Yan, Y. J., and Huang, H. T. (2004). "Chemical elemental characteristics of biomass fuels in China," *Biomass Bioenerg.* 27(2), 119-130.

- Moreau, C., Belgacem, M. N., and Gandini, A. (2004). "Recent catalytic advances in the chemistry of substituted furans from carbohydrates and in the ensuing polymers," *Top. Catal.* 27(1-4), 11-30.
- Nordstierna, L., Lande, S., Westin, M., Karlsson, O., and Furo, I. (2008). "Towards novel wood-based materials: Chemical bonds between lignin-like model molecules and poly (furfuryl alcohol) studied by NMR," *Holzforschung* 62(6), 709-713.
- Pandey, K. (1999). "A study of chemical structure of soft and hardwood and wood polymers by FTIR spectroscopy," *J. Appl. Polym. Sci.* 71(12), 1969-1975.
- Pranger, L., and Tannenbaum, R. (2008). "Biobased nanocomposites prepared by in situ polymerization of furfuryl alcohol with cellulose whiskers or montmorillonite clay," *Macromolecules* 41(22), 8682-8687.
- Rowell, R. M. (2005). "Chemical modification of wood," in: *Handbook of Wood Chemistry and Wood Composites*, R. M. Rowell (ed.), CRC Press, Boca Raton, FL, pp. 381.
- Schneider, M. H., Phillips, J. G., and Lande, S. (2000). "Physical and mechanical properties of wood polymer composites," *J. For. Eng.* 11(1), 83-89.
- Shi, J., Li, J., Zhou, W., and Zhang, D. (2007). "Improvement of wood properties by urea-formaldehyde resin and nano-SiO<sub>2</sub>," *Front. For. China* 2(1), 104-109.
- Stamm, A. J. (1977). "Dimensional stabilization of wood with furfuryl alcohol resin," *Wood Technology: Chemical Aspects, ACS Symposium Series 43, Washington DC*, pp. 141-149.
- Sun, R., Fang, J., Tomkinson, J., Geng, Z., and Liu, J. (2001). "Fractional isolation, physico-chemical characterization and homogeneous esterification of hemicelluloses from fast-growing poplar wood," *Carbohyd. Polym.* 44(1), 29-39.
- Sun, S. L., Wen, J. L., Ma, M. G., Li, M. F., and Sun, R. C. (2013). "Revealing the structural inhomogeneity of lignins from sweet sorghum stem by successive alkali extractions," *J. Agr. Food Chem.* 61(18), 4226-4235.
- Thygesen, L. G., and Elder, T. (2009). "Moisture in untreated, acetylated, and furfurylated Norway spruce monitored during drying below fiber saturation using time domain NMR," *Wood Fiber Sci.* 41(2), 194-200.
- Wu, G. F., Jiang, Y. F., Qu, P., Lang, Q., and Pu, J. (2010). "Effect of chemical modification and hot-press drying on poplar wood," *BioResources* 5(4), 2581-2590.
- Xue, F., and Zhao, G. (2008). "Optimum preparation technology for Chinese fir wood/Ca-montmorillonite (Ca-MMT) composite board," *For. Stud. China* 10(3), 199-204.
- Zavadskii, A. (2004). "X-ray diffraction method of determining the degree of crystallinity of cellulose materials of different anisotropy," *Fibre Chem.* 36(6), 425-430.

Article submitted: May 11, 2014; Peer review completed: August 1, 2014; Revised version received and accepted: August 14, 2014; Published: August 18, 2014.